

Force transmission

Farhang Radjai*, Stéphane Roux**

* *Laboratoire de Mécanique et Génie Civil, Université Montpellier 2, CNRS, Place Eugène Bataillon, 34095 Montpellier cedex 05, France.*

** *LMT-Cachan, (ENS Cachan/CNRS/UPMC/PRES UniverSud Paris) 61, Avenue du Président Wilson, 94235 Cachan cedex.*

1 Introduction

Granular disorder and steric exclusions lead to a strongly inhomogeneous distribution of contact forces in granular media under quasistatic loading (Liu and Jaeger [1995], Radjai et al. [1996], Jaeger and Nagel [1996], Herrmann and Luding [1998], Mueth et al. [1998], Lovol et al. [1999], Bardenhagen et al. [2000], Roux and Radjai [2001], Silbert et al. [2002a], Majmudar and Behringer [2005]). These force inhomogeneities in granular assemblies were first observed optically in packings of photoelastic particles which have the property to develop birefringence on the application of stress (Dantu [1957]). The carbon paper technique was used later to record the force prints at the boundaries of a granular packing (Jaeger and Nagel [1996]). It was found that the forces have a nearly decreasing exponential distribution. The inhomogeneous transmission of forces is interesting as it contradicts somehow the high degree of uniformity in density due to close packing. This is because the forces are transmitted only through interparticle contacts, and are thus determined by the specific features of granular texture.

Later, numerical simulations by the contact dynamics method provided detailed evidence for force chains, the organization of the force network in strong and weak networks, and the exponential distribution of strong forces (Radjai and Roux [1995], Radjai et al. [1998]). Moreover, the force probability density functions (pdf's) from simulations showed that the weak forces (below the average force) in a sheared granular system have a nearly uniform or decreasing power law shape in agreement with refined carbon paper experiments (Radjai et al. [1996], Mueth et al. [1998]).

Further experiments and numerical simulations have shown that the exponential falloff of strong forces is a robust feature of force distribution in granular

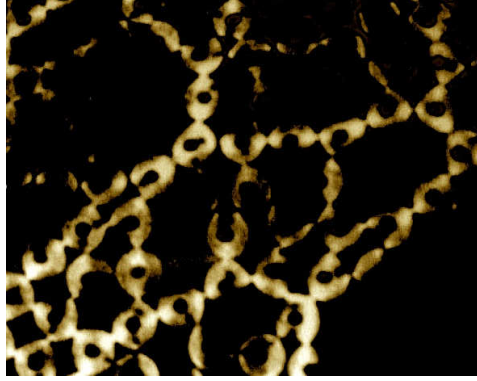


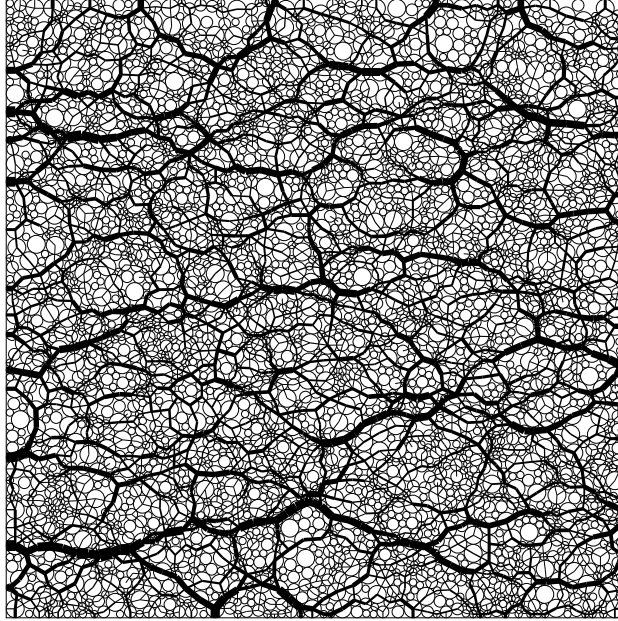
Fig. 1. Photoelastic image of a small assembly of disks.

media both in two and three dimensions. In contrast, the weak forces are sensitive to the details of the preparation method or the internal state of the packing (Mueth et al. [1998], Radjai et al. [1999], Erikson et al. [2002], Antony [2001], Blair et al. [2001], Mueggenburg et al. [2002], Silbert et al. [2002b], Majmudar and Behringer [2005], Azma et al. [2007]). A remarkable aspect of weak forces is that their number does not vanish as the force falls to zero (Radjai and Roux [1995], Metzger [2004]). Several theoretical models have been proposed allowing to relate the exponential distribution of forces to granular disorder combined with the condition of force balance for each particle (Liu and Jaeger [1995], Coppersmith et al. [1996]). Recently, the force pdf's were derived for an isotropic system of frictionless particles in two dimensions from a statistical approach assuming a first shell approximation (one particle with its contact neighbors) (Metzger [2004]).

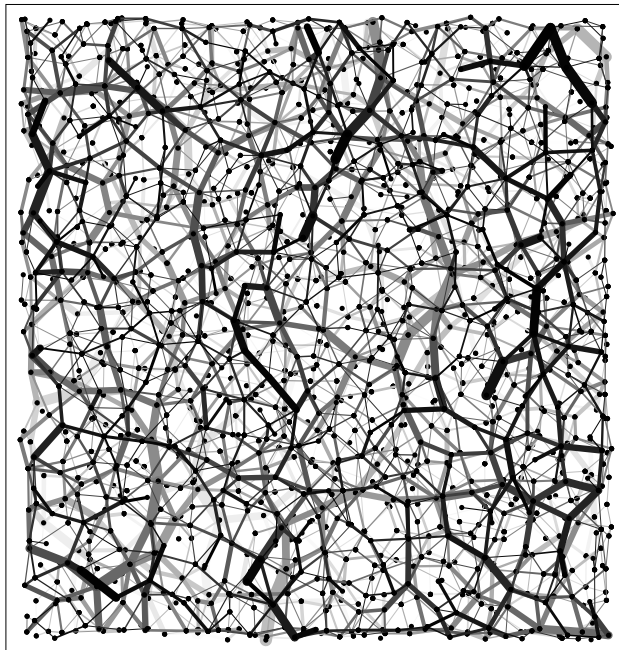
We analyze below the distributions and correlations of contact forces from numerical simulations. A quantitative description of the force distributions and their link with granular texture reveals the *bimodal transmission* of stresses in granular media that will also be briefly presented.

2 Probability density functions

Figure 1 shows one example of a photoelastic image of stresses where the most stressed particles and contacts appear as bright zones. These zones form filamentary patterns that correspond to force chains often spanning several particle diameters. The less bright and dark regions represent the weakly stressed particles and contacts screened as a result of arching. The numerical simulations both in 2D and 3D reveal similar force maps. A 2D packing is displayed in Fig. 2 where the normal forces are encoded as the thickness of branch vectors. In the same figure the force network in a thin layer for a 3D packing of spherical particles subjected to axial compression is shown. Strong force chains are easily distinguished in both cases. The strongest chains have a



(a)



(b)

Fig. 2. The force network in a 2D packing of disks (a) and in a thin layer cut inside a 3D packing of spherical particles (b). The line thickness is proportional to the normal force. The gray level in the 3D system represents the field depth.

linear aspect and they are mostly parallel to the axis of compression (vertical).

Figure 3 displays the radial correlation function $K(r)$ of normal forces in a 2D packing of weakly polydisperse disks (a factor 2 between largest and smallest

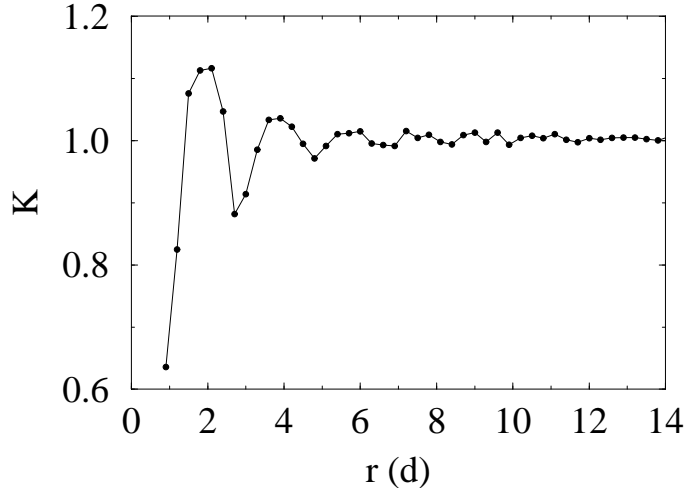


Fig. 3. Radial correlation function K of normal forces for increasing distance r in units of mean particle diameter d between contacts.

diameters). It is defined by

$$K(r) = \frac{\sum_{i=1}^{N_c} \sum_{j=i+1}^{N_c} \delta(r_{ij} - r) f_i f_j}{\langle f \rangle^2 \sum_{i=1}^{N_c} \sum_{j=i+1}^{N_c} \delta(r_{ij} - r)}, \quad (1)$$

where N_c is the number of contacts, r_{ij} is the distance between two contacts i and j , f_i and f_j are the corresponding normal forces, and $\langle f \rangle$ is the average normal force. The Kronecker function δ is equal to 1 when its argument is zero, and 0 otherwise. When there are no correlations, we have $K = 1$. The deviations from $K = 1$ reflect thus the positive and negative correlations. The peaks result from local ordering of the particles and we see that the correlations persist as far as 10 times the mean particle diameter d even though this is only an average over all directions. The actual lengths involved in the network of force chains, as shown in Fig. 2, can be larger.

Figure 4 shows the probability density functions (pdf's) of normal forces f_n for two isotropic samples simulated by molecular dynamics and contact dynamics methods (Richefeu et al. [2008]). The forces are normalized by the average force $\langle f_n \rangle$. The two pdf's have the same shape characterized by an exponential falloff for large forces, a small peak for a force slightly below the average force and a finite value at zero force. The position of the peak is not the same in the two distributions but the exponents of the exponential falloff are the same within statistical precision of the data: $P(f_n) \propto e^{-\beta f_n / \langle f_n \rangle}$ with $\beta \simeq 1.4$.

The observed shape of force pdf's is unique in two respects: (1) the exponential part reflects the presence of very large forces in the system often appearing in a correlated manner in the form of force chains; (2) the nonvanishing density of weak forces, with a proportion of $\simeq 60\%$ of contact forces below the average

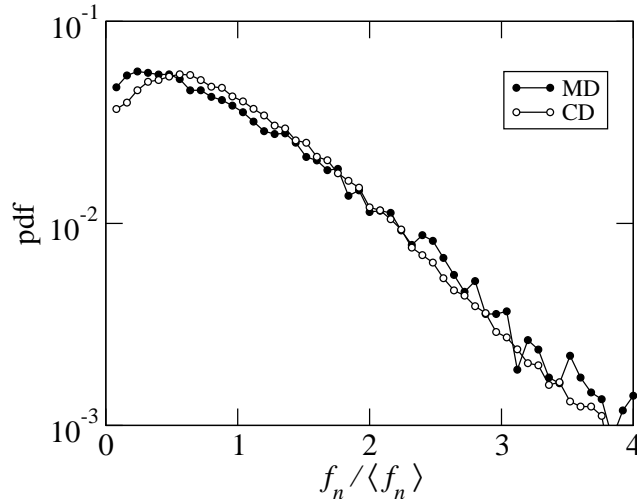


Fig. 4. Probability density functions of normal forces in two isotropic samples of spherical particles simulated by molecular dynamics and contact dynamics methods.

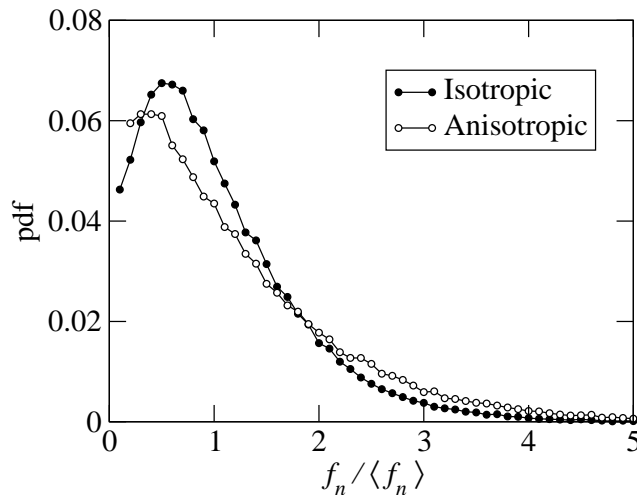


Fig. 5. Probability density functions of normal forces in a sample of spherical particles after isotropic compaction (isotropic state) and following triaxial compression (anisotropic state).

force, means that the stability of force chains is ensured by a large number of vanishingly small forces (Radjai et al. [1998, 1999]). The large number of contacts transmitting very weak forces is a signature of the arching effect.

Figure 5 shows the normal force pdf's in contact dynamics simulations for the same system of spherical particles at the isotropic state (sample S_1) and at an anisotropic state obtained by triaxial compression (sample S_2). The effect of anisotropy is to reinforce the force inhomogeneity by increasing the relative densities of both strong and weak forces (Antony [2001], Radjai et al. [2001], Richefeu et al. [2008]). However, the exponent β remains nearly unchanged whereas the small peak near the average force disappears and the distribution of weak forces tends to become nearly uniform (Radjai et al. [1999]).

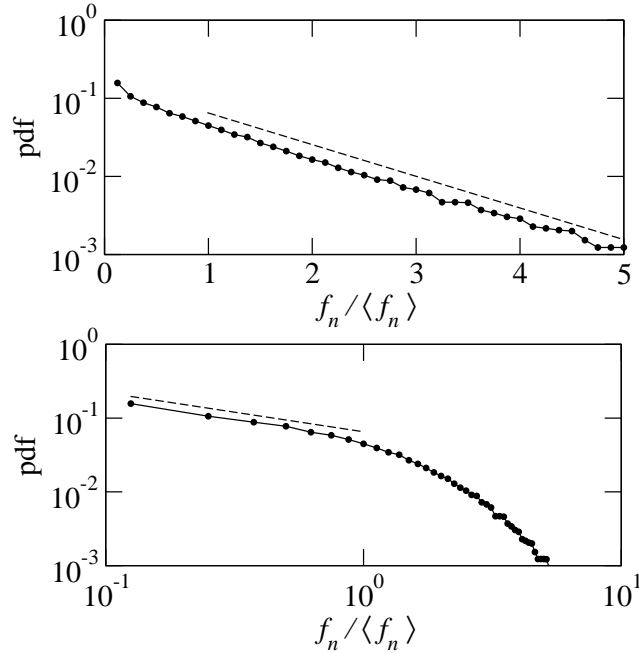


Fig. 6. Probability density functions of normal forces in an isotropic sample of polyhedral particles on log-linear and log-log scales.

The distribution of weak forces is also dependent on particle shapes and sizes. Fig. 6 shows the distribution of normal forces in a sample of polyhedral particles in a dense isotropic state (Azéma et al. [2008]). We again observe the exponential tail of strong forces together with a decreasing power law distribution for weak forces: $P(f_n) \propto (f_n/\langle f_n \rangle)^{-\alpha}$. It seems thus that the angular particle shape increases considerably the number of very weak forces by enhancing the arching effect. The latter affects also the value of the exponent β reduced to 0.97 compared to 1.4 for spherical particles. In this way, the force chains are stronger but less in number.

Figure 7 shows the normal force pdf's for increasingly larger particle size span (Voivret [2008]). We see that the probability density becomes broader with increasing size span s . The weak forces have a clear power law behavior with increasing exponent α . This power-law behavior can be attributed to a “cascade” mechanism from the largest particles “capturing” strongest force chains down to smaller forces carried by smaller particles. A map of normal forces in a highly polydisperse packing ($s = 0.96$) simulated by the contact dynamics method is shown in Fig. 8. A large number of rattlers, i.e. particles not engaged in the force network, can be observed. Although these particles represent a small volume fraction of the sample, their absence from the force-bearing network contributes to force inhomogeneity.

Hence, the distribution of normal forces can be approximated by the following

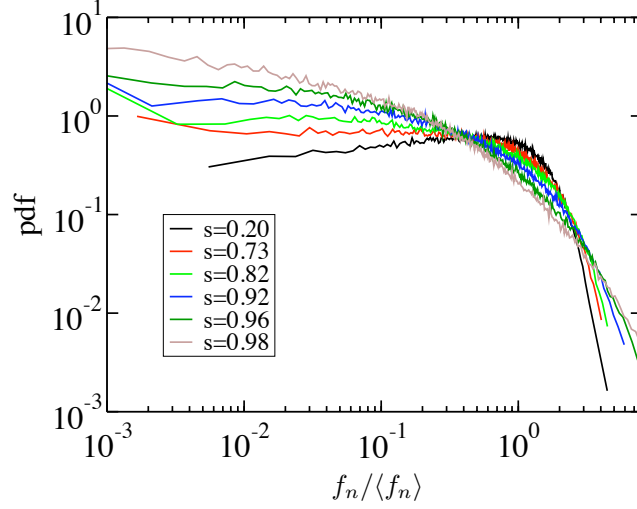


Fig. 7. Probability density functions of normal forces for increasing span s of particle diameters.

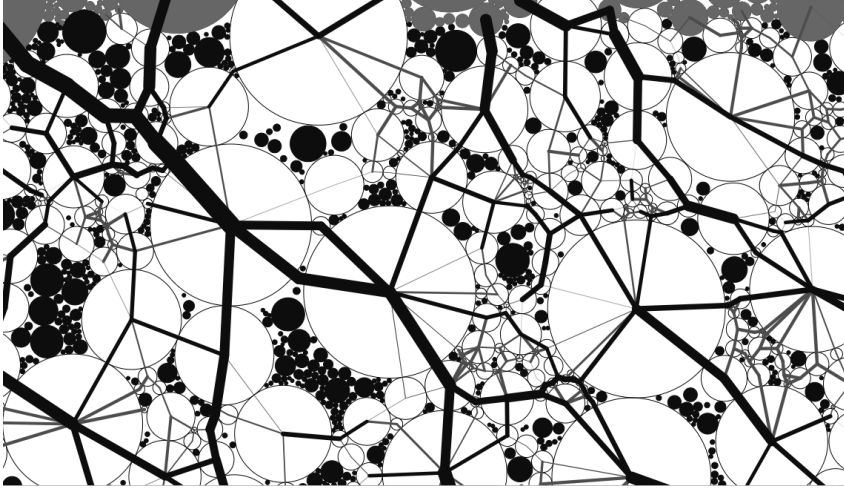


Fig. 8. A map of normal forces in a highly polydisperse system with a uniform size distribution by particle volume fractions. The black particles are “rattlers” excluded from the force-bearing network.

form:

$$P(f_n) = \begin{cases} A \left(\frac{f_n}{\langle f_n \rangle}\right)^{-\alpha} & f_n / \langle f_n \rangle < 1 \\ A e^{\beta(1-f_n/\langle f_n \rangle)} & f_n / \langle f_n \rangle > 1 \end{cases} \quad (2)$$

where k is the normalization factor given by

$$\frac{1}{A} = \frac{1}{1-\alpha} + \frac{1}{\beta} \quad (3)$$

Moreover, considering the mean force $\langle f_n \rangle$ as the point of cross-over between

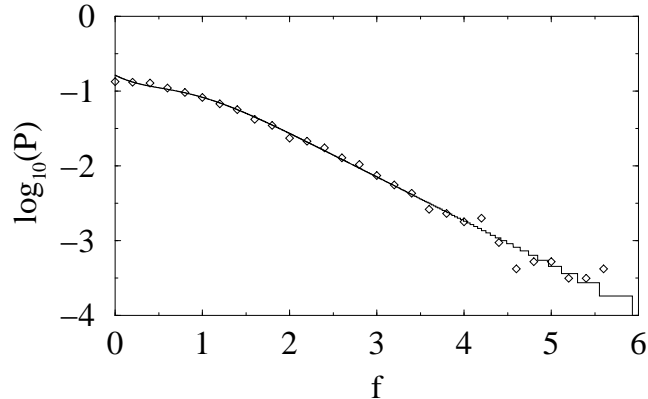


Fig. 9. The probability density of normal forces in a sheared packing of disks fitted by the function [5].

the two parts of the distribution, we get the following relation between the exponents:

$$\beta^2 = (1 - \alpha)(2 - \alpha) \quad (4)$$

Note that the nearly uniform distribution of static forces in the case of sheared circular particles is recovered by setting $\alpha = 0$ in equation (2). Then, from equation [4] we get $\beta = \sqrt{2} \simeq 1.4$ which is the value we found for the distribution of forces in sheared packings of spheres. For this system, the following fitting form was proposed (Mueth et al. [1998]):

$$P(f) = a (1 - be^{-f^2})e^{-\beta f} \quad (5)$$

where $f = f_n / \langle f_n \rangle$. Fig. 9 shows that this form with $b = 0.6$ and $\beta = 1.35$ fits excellently our data, as well, except for $f_n \rightarrow 0$. Actually, a slight increase in P was observed in the experiments as f_n decreased towards zero. As argued by Mueth et al., the above function for the range of weak forces provides a fit essentially indistinguishable from a power law $f_n^{-\alpha}$ as long as α is positive and close to zero (Mueth et al. [1998]).

The presence of cohesive bonding between particles does not alter the inhomogeneous aspect of forces as a result of the common granular texture. However, in contrast to cohesionless media, the distribution of weak compressive forces is affected by tensile forces (Radjai et al. [2001]). In wet granular media in the pendular state (liquid bonds localized in the contact zones between particles), the tensile action of capillary bonds bridging the gaps between neighboring particles gives rise to a network of self-equilibrated forces that lead to particle aggregation and enhanced shear strength in wet granular media (Richefeu et al. [2006, 2007]).

The role of the tail of force distributions and the required statistical precision

depend on the nature of the macroscopic phenomenon considered. For the stress state, a linear size of nearly 10 particle diameters seems to be relevant. For example, in numerical simulations the shear strength is often well-defined for a 2D system composed of 100 disks (increasing to ≈ 500 particles in the presence of rigid walls). For the rheology, involving particle displacements and friction mobilization, the relevant length scales are far larger, as we saw for fluctuating particle displacements in section ???. In the same manner, in a cohesive granular material, the tensile strength is dictated by the highest level of tensile forces rather than the mean force, and finite-size effects are important (Richefeu et al. [2006, 2007]). The exponential falloff is also observed in cohesive granular packings for both compressive and tensile strong forces (Radjai et al. [2001], Richefeu et al. [2007], Topin et al. [2007]). As in molecular solids, the effective tensile strength is generally far below the “theoretical strength” based on the mean stress.

2.1 Bimodal character of stress transmission

In this section, we evaluate various average variables such as the fabric anisotropy and shear stress (in a sheared packing) for subsets of contacts with a given absolute value of the force. Thereby important aspects of the inhomogeneity of the system can be taken into account. For example, the contribution of contact chains with strong forces may be evaluated separately from the weak contacts (Radjai et al. [1998]). This analysis proceeds by considering the subset of contacts which carry a force below a cutoff force $\xi \langle f_n \rangle$. This subset is referred to as the “ ξ -network”. The variation of a quantity evaluated for the “ ξ -network” as ξ is varied from 0 to its maximal value in the system, provides its correlation with the contact force.

For the calculation of the stress tensor, we consider the (tensorial) internal moment M^i of each particle i defined by (Moreau [1997], Staron and Radjai [2005]):

$$M_{\alpha\beta}^i = \sum_{c \in i} f_{\alpha}^c r_{\beta}^c \quad (6)$$

where f_{α}^c is the α component of the force exerted on particle i at the contact c , r_{β}^c is the β component of the position vector of the same contact c , and the summation runs over all contacts c of neighboring particles with the particle i (noted here briefly by $c \in i$). It can be shown that the internal moment of a collection of rigid particles is the sum of the internal moments of individual particles. The stress tensor σ for a packing of volume V is simply given by

(Moreau [1997], Staron and Radjai [2005]):

$$\sigma_{\alpha\beta} = \frac{1}{V} \sum_{i \in V} M_{\alpha\beta}^i = \frac{1}{V} \sum_{c \in V} f_{\alpha}^c \ell_{\beta}^c \quad (7)$$

Remark that the first summation runs over the particles whereas the second summation involves the contacts in the volume V with each contact appearing once.

Under triaxial conditions with compression along the axe 1, we have $\sigma_1 \geq \sigma_2 = \sigma_3$, where the σ_k are the stress principal values. In 3D, we define the mean stress p and stress deviator q by

$$p = \frac{1}{3}(\sigma_1 + \sigma_2 + \sigma_3) \quad (8)$$

$$q = \frac{1}{3}(\sigma_1 - \sigma_3) \quad (9)$$

For a system of perfectly rigid particles, the stress state is characterized by the mean stress p and normalized shear stress q/p . Notice that the corresponding strain variables in 3D are $\varepsilon_p = \varepsilon_1 + \varepsilon_2 + \varepsilon_3$ and $\varepsilon_q \equiv \varepsilon_1 - \varepsilon_3$, such that the input power is simply given by $W = p\varepsilon_p + 2q\varepsilon_q$ in 3D. In 2D, we set $p = (\sigma_1 + \sigma_2)/2$, $q = (\sigma_1 - \sigma_2)/2$, $\varepsilon_p = \varepsilon_1 + \varepsilon_2$ and $\varepsilon_q = \varepsilon_1 - \varepsilon_2$. The corresponding power in 2D is $W = p\varepsilon_p + q\varepsilon_q$.

Since the stress tensor can be calculated for the “ ξ -network”, the normalized stress deviator $q(\xi)/p$ may be evaluated and plotted as a function of ξ . In the same way, from the evaluation of the fabric tensor, we get the anisotropy $a(\xi)$ which corresponds to the fabric anisotropy of the ξ -network. The plot of $q(\xi)/p$ is shown in Fig. 10 for the samples of sheared disks S1 and sheared polygons S2 of Fig. ???. In both samples, the stress deviator is nearly zero for $\xi < 1$, i.e. for the normal forces below the average force. This means that the shear stress is almost totally sustained by the “strong” contact network, defined by $\xi > 1$, for the pentagon packing as well as for the disk packing. Fig. 11 shows the fabric anisotropy $a'(\xi)$ as a function of ξ in the samples S1 and S2. By definition, a positive value of a' corresponds to the major principal stress direction whereas a negative value corresponds to the orthogonal direction. We see that the direction of anisotropy is orthogonal to the principal stress direction ($a' < 0$) for the weak contact network defined by $\xi < 1$. This “orthogonal” anisotropy of the weak forces is more important in the pentagon packing compared to the disk packing, and, as shown in the inset to Fig. 11, it is mainly due to “very weak” forces. When ξ is increased beyond 1, corresponding to the mean normal force $\langle f_n \rangle$, a' becomes less negative and finally changes sign, showing that the strong contacts are preferentially parallel to the principal axis. These strong contacts are less than 40% of all contacts, but their positive contribution to a'

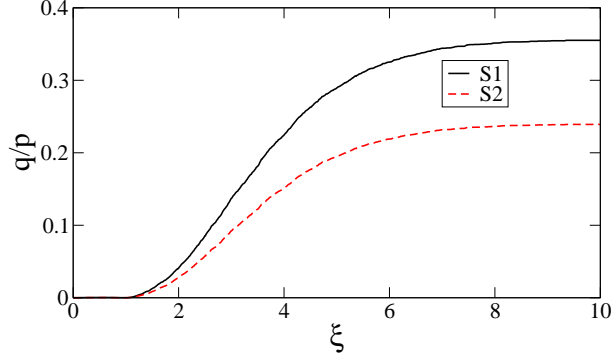


Fig. 10. Partial stress deviator $q(\xi)/p$ as a function of force cutoff ξ for the samples S1 and S2.

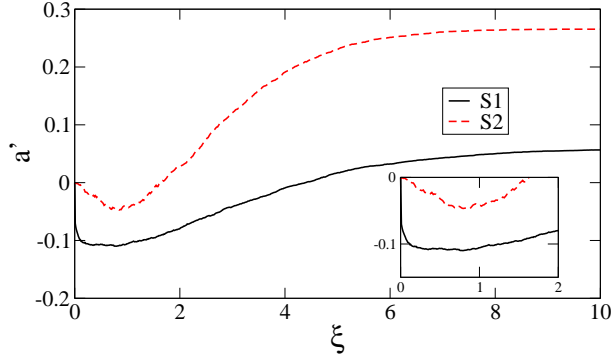


Fig. 11. Partial fabric anisotropy $a'(\xi)$ as a function of force cutoff ξ in the samples S1 and S2.

overcompensates the negative contribution of weak contacts. For large ξ , the partial anisotropy approaches the fabric anisotropy of the whole system.

In this way, the stress tensor can be split into two contributions:

$$\sigma = p_w I + \sigma_s, \quad (10)$$

where p_w is the (isotropic) pressure in the weak phase, I stands for identity tensor and σ_s represents the stress tensor carried only by the strong phase. The simulations show that in a weakly polydisperse packing $p_w \simeq 0.3p$ (Radjai and Wolf [1998]). These observations suggest that force chains in a macroscopically homogeneous granular system can be identified with the strong force network comprising at most 40% of contacts, carrying 70% of the total pressure, and carrying the whole shear stress.

The weak and strong networks are displayed in Fig. 12. Fig. 13 shows the proportion of sliding contacts in the ξ network as a function of ξ . We see that nearly all sliding contacts belong to the strong network. In other words, almost the whole dissipation by friction occurs at contacts bearing a force lower than the average force. Almost all contacts with a force above the average (force

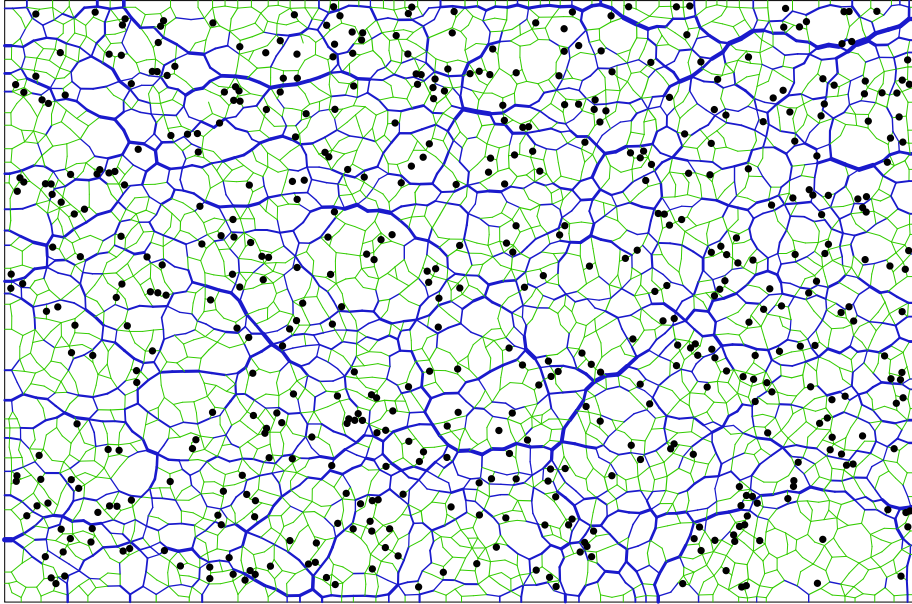


Fig. 12. The force-bearing network of contacts in a biaxially compressed system of 4000 disks. The line thickness is proportional to the normal force. The strong and weak forces are shown in dark and light colors, respectively. The sliding contacts are marked by small filled circles.

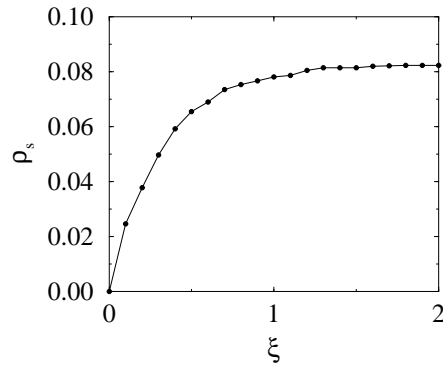


Fig. 13. Proportion of sliding contacts as a function of force cutoff.

chains) are thus rolling contacts.

In summary, the average force in a granular medium, both in 2D and 3D, is a characteristic force separating two complementary phases: 1) A *strong* phase composed of contacts carrying forces above the average force and 2) A *weak* phase composed of contacts carrying forces below the average force. The strong phase carries the whole deviatoric load, while the weak phase contributes only to the average pressure. All contacts within the strong phase are nonsliding, whereas nearly the whole dissipation due to sliding takes place inside the weak phase. The strong phase carries a partial fabric anisotropy induced by shear, but it gives rise to a weak anisotropy inside the weak phase with a privileged direction orthogonal to the major principal stress direction. This orthogonal anisotropy suggests that the weak contacts prop the strong force chains and

enhance in this way the force anisotropy.

2.2 Force anisotropy

In photoelastic experiments, it is clearly observed that the force chains are mainly oriented along the major principal stress direction. This observation can be described, as in the case of the angular proportions of contacts and average branch vector lengths, by defining average normal and tangential forces $\langle f_n \rangle(\vec{n})$ and $\langle f_t \rangle(\vec{n})$ as a function of \vec{n} (or \vec{n}'):

$$\langle f_n \rangle(\vec{n}) = \frac{1}{N_c(\vec{n})} \sum_{c \in \mathcal{A}(\vec{n})} f_n^c \quad (11)$$

$$\langle f_t \rangle(\vec{n}) = \frac{1}{N_c(\vec{n})} \sum_{c \in \mathcal{A}(\vec{n})} f_t^c \quad (12)$$

Figure 14 shows the functions $\langle f_{n'} \rangle(\vec{n}')$ and $\langle f_{t'} \rangle(\vec{n}')$ for the samples S'1 and S'2 of polyhedral and spherical particles under triaxial compression as a function of the branch vector orientations (Azéma et al. [2008]). The simulation data are well fit by the harmonic functions

$$\langle f_{n'} \rangle(\vec{n}') = f_m \{ 1 + a_{n'} [3 \cos^2(\theta' - \theta_{n'}) - 1] \} \quad (13)$$

$$\langle f_{t'} \rangle(\vec{n}') = f_m a_{t'} \sin 2(\theta' - \theta_{t'}) \quad (14)$$

where f_m is the average force, and $a_{n'}$ and $a_{t'}$ are the radial and orthoradial force anisotropies. We see that the radial force anisotropy $a_{n'}$ is much higher in the polyhedra packing than in the sphere packing. A detailed analysis shows that this enhanced force anisotropy is a consequence of the presence of face-face contacts between polyhedra allowing for longer strong force chains. Hence, the aptitude of the polyhedra packing to develop large force anisotropy is correlated with particle shape rather than with fabric anisotropy. The orthoradial force anisotropy $a_{t'}$ has a similar behavior except that it takes considerably higher values in the case of polyhedra compared to spheres.

The general form [13 and 14] of angular force distributions is related to the tensorial nature of the Cauchy stress. Indeed, under axisymmetric boundary conditions, we have

$$\sigma_n(\vec{n}) = p \left\{ 1 + \frac{q}{p} [3 \cos^2(\theta - \theta_\sigma) - 1] \right\} \quad (15)$$

$$\sigma_t(\vec{n}) = p \frac{q}{p} \sin 2(\theta - \theta_\sigma) \quad (16)$$

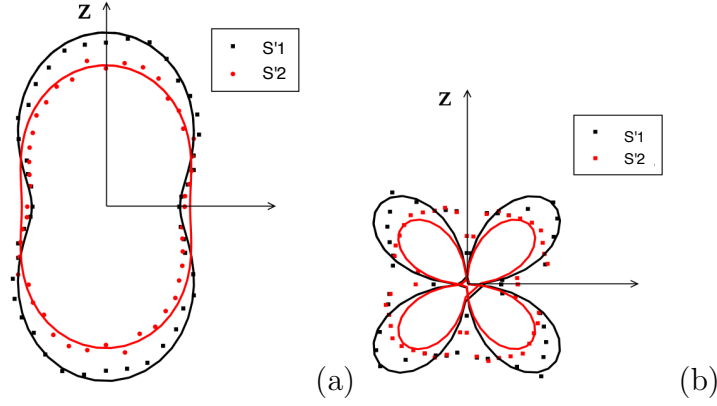


Fig. 14. Polar representation of angular force averages as a function of radial unit vectors in the samples S'1 and S'2 of polyhedral and spherical particles simulated by the contact dynamics method.

where \vec{n} is the space direction with zenith angle θ , $\sigma_n = \sigma_{ij}n_i n_j$, $\sigma_t = \sigma_{ij}n_i t_j$ and θ_σ is the principal stress direction. The comparison between these equations and the equations [13 and 14] suggest that the normalized stress deviator q/p is dependent on a_n (or $a_{n'}$) and a_t (or $a_{t'}$). More generally at a given state, q/p depends both on the force anisotropies a_n and a_t and texture anisotropies a and a_l . The differences between the corresponding phases θ_c , θ_l , θ_n and θ_t are important for general loading paths. But, during a monotonic deformation these privileged directions are nearly coincident, and under axisymmetric conditions and at leading order in anisotropies, the following relations can be established (Azéma et al. [2008]):

$$p \simeq n_c \ell_m f_m \quad (17)$$

$$\frac{q}{p} \simeq \frac{2}{5} (a + a_l + a_n + a_t) \quad (18)$$

where $n_c \equiv N_c/V$ is the number density of the contacts. The corresponding relation in 2D is $q/p = 0.5(a + a_l + a_n + a_t)$. These relations show clearly that the shear strength of a granular material depends on its aptitude to develop fabric and force anisotropies. Depending on the particle shape and sizes, the dominant term can be different. For example, the force anisotropies a_n and a_t depend mainly on the angular particle shape whereas the fabric anisotropies are mostly dependent on polydispersity and elongated particle shape.

References

- S. J. Antony. Evolution of force distribution in three-dimensional granular media. *Phys Rev E*, 63(1 Pt 1):011302, Jan 2001.
- E. Azéma, G. Saussine, and F. Radjai. Quasistatic rheology, force transmis-

- sion and fabric properties of a packing of irregular polyhedral particles. *Mechanics of Materials*, to appear., 2008.
- Emilien Azma, Farhang Radja, Robert Peyroux, and Gilles Saussine. Force transmission in a packing of pentagonal particles. *Phys Rev E Stat Nonlin Soft Matter Phys*, 76(1 Pt 1):011301, Jul 2007.
- S. G. Bardenhagen, J. U. Brackbill, and D. Sulsky. Numerical study of stress distribution in sheared granular material in two dimensions. *Phys. Rev. E*, 62:3882–3890, 2000.
- D. L. Blair, N. W. Mueggenburg, A. H. Marshall, H. M. Jaeger, and S. R. Nagel. Force distributions in three-dimensional granular assemblies: effects of packing order and interparticle friction. *Phys Rev E Stat Nonlin Soft Matter Phys*, 63(4 Pt 1):041304, Apr 2001.
- S. N. Coppersmith, C.-h. Liu, S. Majumdar, O. Narayan, and T. A. Witten. Model for force fluctuations in bead packs. *Phys. Rev. E*, 53(5):4673–4685, 1996.
- P. Dantu. Contribution à l'étude mécanique et géométrique des milieux pulvérulents. In *Proc. Of the 4th International Conf. On Soil Mech. and Foundation Eng.*, volume 1, pages 144–148, London, 1957. Butterworths Scientific Publications.
- J. Michael Erikson, Nathan W Mueggenburg, Heinrich M Jaeger, and Sidney R Nagel. Force distributions in three-dimensional compressible granular packs. *Phys Rev E Stat Nonlin Soft Matter Phys*, 66(4 Pt 1):040301, Oct 2002.
- H. J. Herrmann and S. Luding. Modeling granular media with the computer. *Continuum Mechanics and Thermodynamics*, 10:189–231, 1998.
- H.M. Jaeger and S.R. Nagel. Granular solids, liquids and gases. *Reviews of Modern Physics*, 68:1259–1273, 1996.
- C.-h. Liu and H. M. Jaeger. Comment on water droplet avalanches. *Phys. Rev. Lett.*, 74(17), 1995.
- G. Lovol, K. Maloy, and E. Flekkoy. Force measurements on static granular materials. *Phys. Rev. E*, 60:5872–5878, 1999.
- T. S. Majmudar and R. P. Behringer. Contact force measurements and stress-induced anisotropy in granular materials. *Nature*, 435(7045):1079–1082, Jun 2005. doi: 1038/nature03805. URL <http://dx.doi.org/1038/nature03805>.
- Philip T Metzger. Comment on "mechanical analog of temperature for the description of force distribution in static granular packings". *Phys Rev E Stat Nonlin Soft Matter Phys*, 69(5 Pt 1):053301; discussion 053302, May 2004.
- J. J. Moreau. Numerical investigation of shear zones in granular materials. In D. E. Wolf and P. Grassberger, editors, *Friction, Arching, Contact Dynamics*, pages 233–247, Singapore, 1997. World Scientific.
- Nathan W Mueggenburg, Heinrich M Jaeger, and Sidney R Nagel. Stress transmission through three-dimensional ordered granular arrays. *Phys Rev E Stat Nonlin Soft Matter Phys*, 66(3 Pt 1):031304, Sep 2002.
- D. M. Mueth, H. M. Jaeger, and S. R. Nagel. Force distribution in a granular

- medium. *Phys. Rev. E*, 57:3164, 1998.
- Radjai and Roux. Friction-induced self-organization of a one-dimensional array of particles. *Phys. Rev. E*, 51(6):6177–6187, Jun 1995.
- F. Radjai and D. E. Wolf. The origin of static pressure in dense granular media. *Granular Matter*, 1:3–8, 1998.
- F. Radjai, D. E. Wolf, M. Jean, and J.J. Moreau. Bimodal character of stress transmission in granular packings. *Phys. Rev. Letter*, 80:61–64, 1998.
- F. Radjai, I. Preechawuttipong, and R. Peyroux. Cohesive granular texture. In P.A. Vermeer, S. Diebels, W. Ehlers, H.J. Herrmann, S. Luding, and E. Ramm, editors, *Continuous and discontinuous modelling of cohesive frictional materials*, pages 148–159, Berlin, 2001. Springer Verlag.
- Farhang Radjai, Michel Jean, Jean-Jacques Moreau, and Stphane Roux. Force distributions in dense two-dimensional granular systems. *Phys. Rev. Lett.*, 77(2):274–, July 1996. URL <http://link.aps.org/abstract/PRL/v77/p274>.
- Farhang Radjai, Stephane Roux, and Jean Jacques Moreau. Contact forces in a granular packing. *Chaos*, 9(3):544–550, Sep 1999. doi: 10.1063/1.166428. URL <http://dx.doi.org/10.1063/1.166428>.
- V. Richefeu, F. Radjai, and M. S. El Youssoufi. Stress transmission in wet granular materials. *Eur. Phys. J. E*, 21: 359–369, Feb 2007. doi: 10.1140/epje/i2006-10077-1. URL <http://dx.doi.org/10.1140/epje/i2006-10077-1>.
- Vincent Richefeu, Moulay Saïd El Youssoufi, and Farhang Radjai. Shear strength properties of wet granular materials. *Phys. Rev. E*, 73(5 Pt 1): 051304, May 2006.
- Vincent Richefeu, Moulay Said El Youssoufi, Emilien Azéma, and Farhang Radjai. Force transmission in dry and wet granular media. *Powder Technology*, In Press:–, 2008. doi: <http://dx.doi.org/10.1016/j.powtec.2008.04.069>. URL <http://www.sciencedirect.com/science/article/B6TH9-4SDX2V6-3/1/54563d4cb3fa3d4e9>
- S. Roux and F. Radjai. Statistical approach to the mechanical behavior of granular media. In H. Aref and J.W. Philips, editors, *Mechanics for a New Millennium*, pages 181–196, Netherlands, 2001. Kluwer Acad. Pub.
- Leonardo E Silbert, Deniz Erta?, Gary S Grest, Thomas C Halsey, and Dov Levine. Analogies between granular jamming and the liquid-glass transition. *Phys Rev E Stat Nonlin Soft Matter Phys*, 65(5 Pt 1):051307, May 2002a.
- Leonardo E Silbert, Gary S Grest, and James W Landry. Statistics of the contact network in frictional and frictionless granular packings. *Phys Rev E Stat Nonlin Soft Matter Phys*, 66(6 Pt 1):061303, Dec 2002b.
- Lydie Staron and Farhang Radjai. Friction versus texture at the approach of a granular avalanche. *Phys Rev E*, 72(4 Pt 1):041308, Oct 2005.
- V. Topin, J-Y. Delenne, F. Radjai, L. Brendel, and F. Mabilbe. Strength and failure of cemented granular matter. *Eur. Phys. J. E*, 23(4):413–429, Aug 2007. doi: 10.1140/epje/i2007-10201-9. URL <http://dx.doi.org/10.1140/epje/i2007-10201-9>.

Charles Voivret. *Texture et comportement des matériaux granulaires à grande polydispersité*. PhD thesis, Université Montpellier 2, 2008.